Spectroscopic ellipsometry study of Cu2ZnSnSe4 bulk crystals

M. León, S. Levcenko, R. Serna, I. V. Bodnar, A. Nateprov, M. Guc, G. Gurieva, N. Lopez, J. M. Merino, R. Caballero, S. Schorr, A. Perez-Rodriguez, and E. Arushanov

Citation: Applied Physics Letters **105**, 061909 (2014); doi: 10.1063/1.4892548
View online: http://dx.doi.org/10.1063/1.4892548
View Table of Contents: http://scitation.aip.org/content/aip/journal/apl/105/6?ver=pdfcov
Published by the AIP Publishing

Spectroscopic ellipsometry study of $Cu_2ZnSnSe_4$ bulk crystals

M. León,[1,a)] S. Levcenko,[2] R. Serna,[3] I. V. Bodnar,[4] A. Nateprov,[5] M. Guc,[5] G. Gurieva,[2] N. Lopez,[1] J. M. Merino,[1] R. Caballero,[1] S. Schorr,[2,6] A. Perez-Rodriguez,[7,8] and E. Arushanov[5]

[1]*Department of Applied Physics M12, Universidad Autónoma de Madrid, Madrid, Spain*
[2]*Helmholtz-Zentrum Berlin fuer Materialien und Energie, Berlin, Germany*
[3]*Laser Processing Group, Instituto de Optica, CSIC, Serrano 121, 28006 Madrid, Spain*
[4]*Department of Chemistry, Belarusian State University of Informatics and Radioelectronics, Minsk, Belarus*
[5]*Institute of Applied Physics, Academy of Sciences of Moldova, Chisinau MD 2028, Moldova*
[6]*Institute of Geological Sciences, Free University Berlin, Malteserstr. 74-100, Berlin, Germany*
[7]*IREC, Catalonia Institute for Energy Research, C. Jardins de les Dones de Negre 1, 08930 Sant Adrià del Besòs (Barcelona), Spain*
[8]*IN2UB, Departament d'Electrònica, Universitat de Barcelona, Martí i Franquès 1, 08028 Barcelona, Spain*

(Received 26 June 2014; accepted 26 July 2014; published online 15 August 2014)

Using spectroscopic ellipsometry we investigated and analyzed the pseudo-optical constants of $Cu_2ZnSnSe_4$ bulk crystals, grown by the Bridgman method, over 0.8–4.5 eV photon energy range. The structures found in the spectra of the complex pseudodielectric functions were associated to E_0, E_{1A}, and E_{1B} interband transitions and were analyzed in frame of the Adachi's model. The interband transition parameters such as strength, threshold energy, and broadening were evaluated by using the simulated annealing algorithm. In addition, the pseudo-complex refractive index, extinction coefficient, absorption coefficient, and normal-incidence reflectivity were derived over 0.8–4.5 eV photon energy range. © *2014 AIP Publishing LLC*.
[http://dx.doi.org/10.1063/1.4892548]

A recent conversion efficiency of nearly 10% has been produced on kesterites $Cu_2ZnSnSe_4$ (CZTSe)-based thin film solar cells.[1,2] In spite of this promising value, there are still some unsolved problems related to the single phase growth and its characterization due to the presence of undesired secondary phases of ternary and/or binary compounds[3–6] and there are only few reports in the literature with experimental information on the fundamental properties of these materials. The investigation of the kesterites optical properties and, in particular, their optical constants, is of great interest for both fundamental and application reasons. Some optical constants data from theoretical *ab-initio* calculations[7–10] and from a few experimental reports on CZTSe polycrystalline thin films[8,9,11] and bulk crystals[12] have already been reported. With the aim of get a better understanding of the optical constants, we have studied the room temperature spectroscopic ellipsometry (SE) of CZTSe bulk crystals, grown by the Bridgman method. The optical measurements were carried out over the photon energy range from 0.8 to 4.5 eV. The determined pseudo-optical constants of the CZTSe quaternary compounds have been modelled using the Adachi's model dielectric function for the electronic interband transitions in the neighbourhood of the critical points (CPs) of the joint density of state function.

CZTSe crystals were grown by the modified Bridgman method. The ingot was prepared by direct reaction of a stoichiometry mixture of Cu, Zn, Sn, Se (all of a minimum purity of 99.999%) in vertical furnace with temperature gradient ~10 °C along furnace axe at ampoules zone. A ~20 g mixture was placed in an 18 mm diameter quartz ampoule covered inside with graphite. Ampoule was sealed under vacuum. The mixture was quickly heated up to 600 °C and kept at 600 °C during 48 h. In next step, mixture was heated at a rate of 50 °C/h to 950 °C, kept at this temperature during 10 h. For the crystallization process temperature was lowered from 950 °C to 600 °C with a rate of 10 °C/h and annealed at this temperature during 2–3 weeks. Next cooling from 600 °C to room temperature was made in switched off furnace mode. Three samples were selected and their composition examined by Energy Dispersive X-ray microanalysis (EDX) measurements (Oxford instruments, model INCA x-sight) inside a Hitachi S-3000N scanning electron microscope. EDX measurements were carried out at 25 kV operating voltage and the Cu K, Zn K, Sn L, and Se K lines were used for quantification. The determined composition is given in Table I. The Cu/Zn+Sn ratio varies from 0.8 to 1.2 and the Zn/Sn ratio lies in the range of 0.9–1.1 in the grown samples. The structural analysis was performed by powder X-ray diffraction (XRD) at room temperature. The data were collected using a PANalytical X'pertPro MPD diffractometer equipped with CuKα radiation ($\lambda = 1.54056$ Å) in a focusing Bragg-Brentano geometry. Even though the samples are out of stoichiometry, the XRD data (Fig. 1) of the CZTSe crystals confirm a good crystallinity quality and show that the

TABLE I. Compositional data (EDX).

$Cu_2ZnSnSe_4$	Cu (at. %)	Zn (at. %)	Sn (at. %)	Se (at. %)	Sn/Zn	Cu/(Sn + Zn)
*S*1	27.10	10.98	13.41	48.51	1.22	1.11
*S*2	28.23	12.76	12.52	46.49	0.98	1.12
*S*3	24.32	15.37	12.53	47.78	0.82	0.87

a)Author to whom correspondence should be addressed. Electronic mail: maximo.leon@uam.es

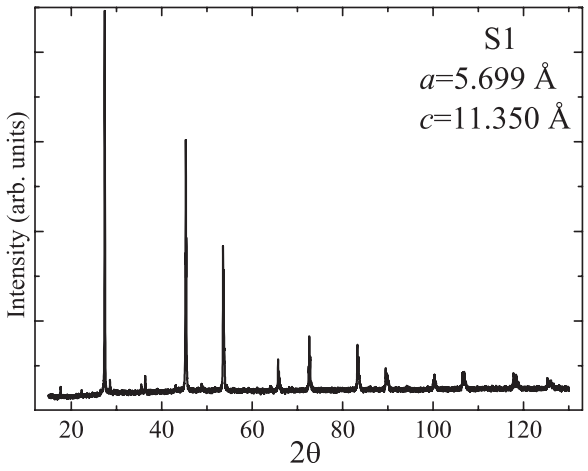

FIG. 1. XRD spectra of CZTSe simple.

samples adopt a tetragonal structure (stannite or kesterite) with no preferential orientation of the polycrystalline grains. Lattice constants were obtained from the Rietveld refinement of the diffraction data using the FullProf suite software.[13]

In order to discard the presence of bynaries or another secondary phases Raman spectra were measured. Raman spectra were carried out using a LabRam HR800-UV Horiba Jobin Yvon spectrometer with a laser excitation source YAG:Nd solid state laser (line 532 nm). Spectra were obtained in backscattering configuration at room temperature; excitation and light collection were done through an Olympus metallographic microscope, with a laser spot on the sample surface of ~1 μm and laser power ~1 mW. Fig. 2 shows a typical Raman spectrum measured on S3 CZTSe sample, together with its fitting with lorentzian curves. All the observed peaks can be interpreted and all Raman active modes can be assigned to those of CZTSe semiconductor[14] and no modes related to possible secondary phases were detected. The low values of the full width on the half maximum (~5 cm^{-1} for the most of the peaks) support the high crystalline quality of the grown samples observed in the XRD analysis.

SE measurements were performed using a variable angle spectroscopic ellipsometer (J.A. Woollam VASE) at room

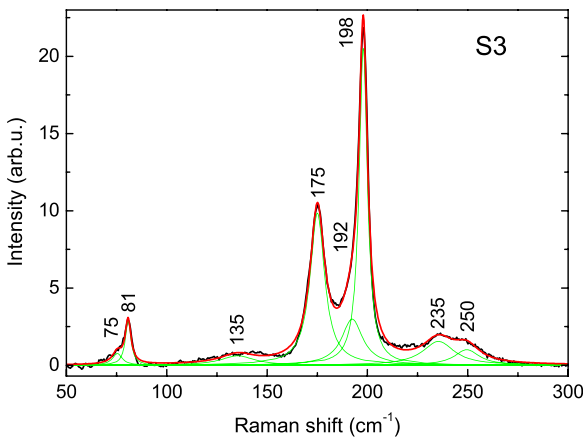

FIG. 2. Raman spectra of CZTSe S3 sample (excitation wavelength 532 nm). Green curves show the Lorentzian curves used to fit the experimental spectrum.

temperature. The ellipsometric parameters were acquired in the photon energy range from 0.8 to 4.5 eV using a step of 0.03 eV, and at three angles of incidence (65°, 70°, and 75°). The samples were polished following the procedure proposed by Albornoz *et al.* in order to minimize the presence of oxides and roughness effects.[15]

The real part $\varepsilon_1(E)$ and the imaginary part $\varepsilon_2(E)$ of the pseudo-dielectric functions of three different CZTSe bulk crystals, determined from ellipsometry measurements by using a two-phase model,[16] are plotted in Fig. 3(a). Even though some discrepancy in the absolute values of $\varepsilon(E)$ function, its shape is identical and reveals clear E_0, E_{1A}, and E_{1B} structures, indicated in Fig. 3(b). The fundamental absorption edge $E_0 = E_g$ is observed near 1 eV in agreement with Chen *et al.*[10] calculations, and high energy features E_{1A} (E_{1B}) are found at about 2.3 (4.0) eV, respectively, in agreement with the previous reports.[8,11,12]

According to the Adachi's model for the dielectric function (MDF), the electronic transitions in the neighborhood of CP contribute to the features of the complex dielectric function $\varepsilon(E)$.[17] We employed this approach and modelled the pseudo-dielectric function of the CZTSe crystals. The experimental pseudo-dielectric function $\varepsilon(E) = \varepsilon_1(E) + \varepsilon_2(E)$ can be well fitted by summing up the contributions from E_0, E_{1A}, and E_{1B} CPs, written as

$$\varepsilon(E) = \varepsilon^{(0)}(E) + \varepsilon^{(1)}(E) + \varepsilon_{1\infty}, \quad (1)$$

where the first and second terms are one-electron contributions at the fundamental gap, E_0 and at high energy transitions, $E_{1\beta}$ ($\beta = A, B$), respectively, and $\varepsilon_{1\infty}$ is an additional constant determined by electronic transitions lying beyond the experimental range.[17] The $\varepsilon^{(0)}(E)$-term corresponds to transitions at the three-dimensional (3D) M_0 CP and read as

$$\varepsilon^{(0)}(E) = AE_0^{-3/2}\chi_0^{-2}(2 - (1+\chi_0)^{1/2} - (1-\chi_0)^{1/2}), \quad (2)$$

with $\chi_0 = (E + i\Gamma_0)/E_0$, where A and Γ_0 are the strength and the damping energy of the E_0 gap, respectively.

The $\varepsilon^{(1)}(E)$ accounts for the E_{1A} and E_{1B} higher transitions at 2D-M_0 and 2D-M_1 CPs, respectively, and is given by

$$\varepsilon^{(1)}(E) = B_{1A}[1 - (E/E_{1A})^2 - i(E/E_{1A})\Gamma_{1A}]^{-1} - B_{1B}\chi_{1B}^{-2}\ln(1 - \chi_{1B}^2), \quad (3)$$

where B_{1A} and Γ_{1A} are the non-dimensional strength and damping constants of the E_{1A} transition and $\chi_{1B} = (E + i\Gamma_{1B})/E_{1B}$, with B_{1B} and Γ_{1B} are the strength and damping energy of the E_{1B} transition.

A simulated annealing (SA) algorithm was used to compute the MDF parameters.[17–19] The objective function[19] was minimized to obtain the unknown MDF parameters through the SA algorithm[18] is

$$F = \sum_{i=1}^{N}\left(\left|\frac{\varepsilon_1(E_i)}{\varepsilon_1^{\text{expt}}(E_i)} - 1\right| + \left|\frac{\varepsilon_2(E_i)}{\varepsilon_2^{\text{expt}}(E_i)} - 1\right|\right)^2, \quad (4)$$

where $\varepsilon_1{}^{\text{expt}}(E_i)$, $\varepsilon_1(E_i)$ $\varepsilon_2{}^{\text{expt}}(E_i)$, $\varepsilon_2(E_i)$ are the experimental and calculated values of the real and imaginary parts of the complex dielectric function at E_i point, respectively, and N

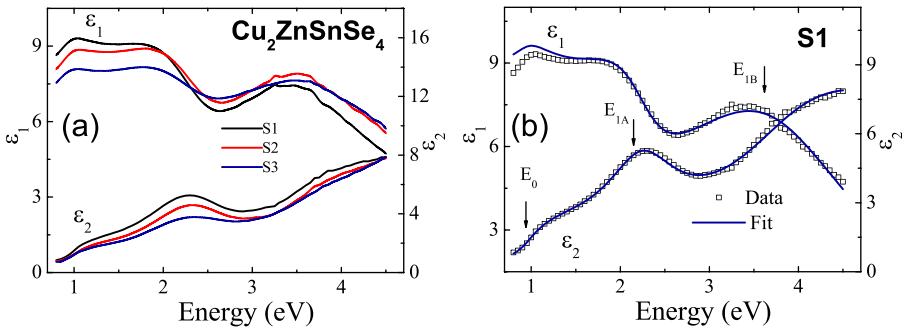

FIG. 3. Pseudodielectric function spectra, real part $\varepsilon_1(E)$ and imaginary part $\varepsilon_2(E)$, of CZTSe samples (a) and numerically calculated (solid lines) using the MDF model and the SA algorithm for S1-sample (b). The obtained values of the transition energies denoted as E_0, E_{1A}, and E_{1B} are indicated by the arrows.

is the number of the experimental points. As an example of the result of the fitting procedure, we depict the calculated $\varepsilon(E)$ for the S1 sample in Fig. 3(b).

The model parameters A, B_{1A}, B_{1B}, E_0, E_{1A}, E_{1B}, Γ_{1A}, Γ_{1B} and $\varepsilon_{1\infty}$ of the interband electronic transitions for the three samples are summarized in Table II. As a consistency check of the MDF calculation, we computed the relative errors, $\Delta\varepsilon_1$ and $\Delta\varepsilon_2$, obtaining values smaller than 2.0% for both real and imaginary parts, respectively (Table II). According to Table II, the main differences in the determined MDF parameters can be found for the strength parameters (A and B_{1A}), differing less in the values of the transition energies of E_0 and E_{1A} structures, which correlates well to the above mentioned similarity of the $\varepsilon(E)$ shape for the studied samples. We assume that the observed differences in the strength parameters are rather related to the difference in the density or size of the grains in the polycrystalline samples than to the quality of the upper surface sample layer, as all of the studied samples were treated in similar way before the ellipsometry measurements. In the case of the E_{1B} structure, changes in both strength and transition energy parameters can be observed in Table II; however, its proximity to the high energy end of the experimental range limits the accuracy of its analysis.

The MDF parameters can be used to determine the value of the high-frequency dielectric constant (ε_∞) by using the formula $\varepsilon_\infty(\lambda \rightarrow \infty) \approx A/(4E_0{}^{1.5}) + B_{1A} + B_{1B} + \varepsilon_{1\infty}$.[20] The found value of ε_∞ lies between 8.87 and 8.07 for the studied CZTSe samples, which is comparable to 8.42 for close related $Cu_2ZnGeSe_4$ semiconductor.[21]

For the band gap transition (E_0 transition) of CZTSe, the calculation yields values of 0.93–0.95 eV (Table II). Recent band structure calculations suggest that E_0 type transition is due to a direct electronic transition at the Γ:(000) point.[7,8] From the absorption measurements, band gap values of 1.0–1.02 eV (Refs. 9, 11, and 12) were found. The possible reasons for the differences between our results and the reported values might be related to the method of the optical measurement and data analysis. First, in previous works, the absorption coefficient was derived only from transmission measurements and the subsequent analysis of the optical data was done in a somewhat simplified way, assuming constant reflectivity. Second, the derived band gap value depends on the selected linear part in Tauc plots. We cannot compare our E_0 values with earlier ellipsometry studies on CZTSe as the band gap feature was not analyzed[8] or even was not measured.[12]

In the higher energy region, we determined values of 2.29–2.32 and 3.73–3.92 eV for E_{1A} and E_{1B} transitions, respectively. These observed transitions might occur at the Z(0, 0, 0.5) point of the first Brillouin zone of the CZTSe.[8] Our results are in fair agreement with the identified transitions at 2.42 and 4.01 eV from ellipsometry in thin films[8] and with 2.45 and 3.94 eV transitions observed by thermoreflectance in bulk.[12] Note that in these previous studies, the authors used an excitonic line shape for the data analysis, while we applied interband electronic transitions from CPs of 2D type to describe the $\varepsilon(E)$ function, in accordance to the typical approach for the $\varepsilon(E)$ function analysis of close related ternary chalcopyrite compounds.[17,22] The exciton feature was only observed in the photoluminescence spectra at liquid helium temperatures for CZTSe thin films,[23] while in the mentioned studies, optical measurements were carried out at a room temperature. Thus, the possible physical reason to use the excitonic contribution to the $\varepsilon(E)$ at 300 K remains to be determined, and not only because this model may give a better agreement for the $\varepsilon(E)$ function description.[8,12]

The pseudo-optical constants such as complex refractive index $n^* = n + ik$, the normal-incidence reflectivity R, and the absorption coefficient α, can be readily derived from the $\varepsilon(E)$ function from well-known equations (see Eqs. (5)–(7) in Ref. 24). In Fig. 4(a), we show n and k for the studied samples, and as an example we show a comparison of the experimental and calculated values of the complex refractive index using the MDF for the S1-sample in Fig. 4(b). Figs. 5(a) and 5(b) show similar plots for α and R pseudo optical constants of CZTSe. The calculated spectra show a good agreement with experimental data.

TABLE II. Model parameter values.

Parameters											Error	
Samples	E_0 (eV)	Γ_0 (eV)	A ($eV^{1.5}$)	E_{1A} (eV)	Γ_{1A}	B_{1A}	E_{1B} (eV)	Γ_{1B} (eV)	B_{1B}	$\varepsilon_{1\infty}$	$\Delta\varepsilon_1$%	$\Delta\varepsilon_2$%
S1	0.95	0.13	4.8	2.29	0.41	1.20	3.73	0.9	6.0	0.37	1.8	1.3
S2	0.95	0.15	4.1	2.32	0.39	0.95	3.84	0.9	6.0	0.55	1.9	1.7
S3	0.93	0.09	2.9	2.31	0.45	0.76	3.92	1.0	6.5	…	1.7	1.4

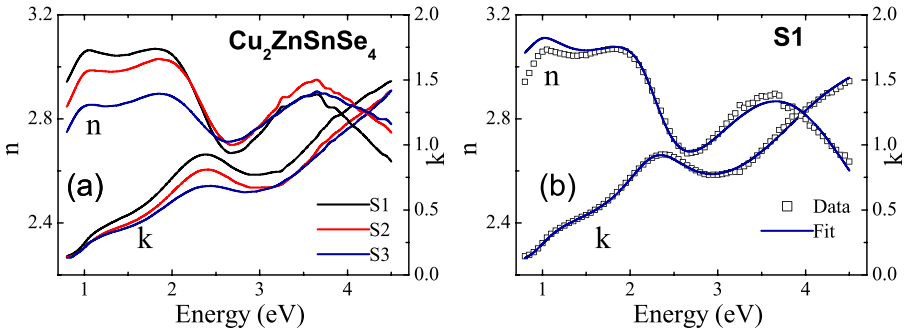

FIG. 4. Experimental spectral dependence of the pseudo-real refraction index n and pseudo-extinction coefficient k of CZTSe samples (a) and numerically calculated (solid lines) using the MDF model and the SA algorithm for S1-sample (b).

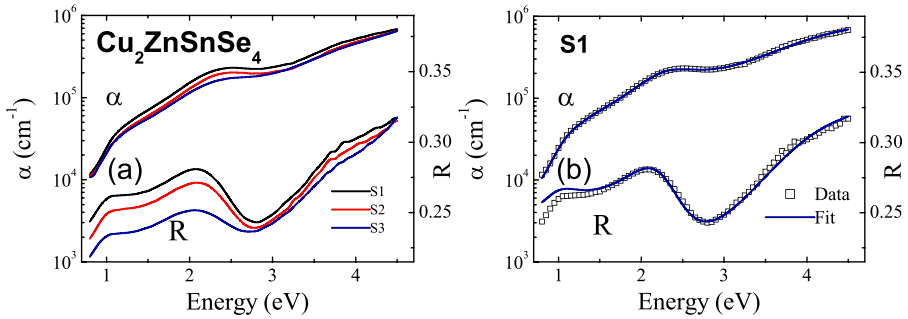

FIG. 5. Experimental spectral dependence of pseudo-absorption coefficient of CZTSe samples (a) and numerically calculated (solid lines) using the MDF model and the SA algorithm for S1-sample (b).

In summary, the room temperature pseudo-optical constants for $Cu_2ZnSnSe_4$ polycrystalline crystals, grown by the modified Bridgman method, have been measured by spectroscopic ellipsometry in the 0.8–4.5 eV photon energy range. Complementary XRD and Raman scattering measurements corroborate the high crystalline quality of the grown samples and suggest the absence in these samples of secondary phases. The optical measurements reveal clear structures which have been attributed to a contribution from the interband transitions in the vicinity of the critical points. The optical spectra have been modelled by using the Adachi's model dielectric function described by E_0, E_{1A}, and E_{1B} interband transitions. The values of the model parameters (strength, threshold energy, and broadening) of the interband transitions were computed by the simulated annealing algorithm. In favour of its application, the reported dielectric function model could be useful for the design and analysis of optoelectronic devices based on the $Cu_2ZnSnSe_4$ material.

This work was supported by projects: Marie Curie-IRSES (PVICOKEST, GA: 269167), FRCFB 13.820.05.11/BF, 14.819.02.17F, TEC2012-38901-C02-01 (Spain) and the institutional Project No. 11.817.05.03A. R.C. acknowledges financial support from Spanish MINECO within the program Ramón y Cajal (RYC-2011-08521).

[1]G. Brammertz, M. Buffiere, S. Oueslati, H. ElAnzeery, K. Ben Messaoud, S. Sahayaraj, C. Koble, M. Meuris, and J. Poortmans, Appl. Phys. Lett. **103**, 163904 (2013).
[2]I. Repins, C. Beall, N. Vora, C. De Hart, D. Kuciauskas, P. Dippo, B. To, J. Mann, W. C. Hsu, A. Goodrich, and R. Noufi, Sol. Energy Mater. Sol. Cells **101**, 154 (2012).
[3]T. Schwarz, O. Cojocaru-Miredin, P. Choi, M. Mousel, A. Redinger, S. Siebentritt, and D. Raabe, Appl. Phys. Lett. **102**, 042101 (2013).
[4]A. Polizzotti, I. L. Repins, R. Noufi, S.-H. Wei, and D. B. Mitzi, Energy Environ. Sci. **6**, 3171 (2013).
[5]R. Djemour, M. Mousel, A. Redinger, L. Gutay, A. Crossay, D. Colombara, P. J. Dale, and S. Siebentritt, Appl. Phys. Lett. **102**, 222108 (2013).
[6]T. Tanaka, T. Sueishi, K. Saito, Q. Guo, M. Nishio, K. M. Yu, and W. Walukiewicz, J. Appl. Phys. **111**, 053522 (2012).
[7]C. Persson, J. Appl. Phys. **107**, 053710 (2010).
[8]S. G. Choi, H. Y. Zhao, C. Persson, C. L. Perkins, A. L. Donohue, B. To, A. G. Norman, J. Li, and I. L. Repins, J. Appl. Phys. **111**, 033506 (2012).
[9]S. Ahn, S. Jung, J. Gwak, A. Cho, K. Shin, K. Yoon, D. Park, H. Cheong, and J. H. Yun, Appl. Phys. Lett. **97**, 021905 (2010).
[10]S. Chen, X. G. Gong, A. Walsh, and S. H. Wei, Appl. Phys. Lett. **94**, 041903 (2009).
[11]L. Gutay, A. Redinger, R. Djemour, and S. Siebentritt, Appl. Phys. Lett. **100**, 102113 (2012).
[12]S. Ozaki and T. Namba, Phys. Status Solidi C **9**, 2403 (2012).
[13]J. Rodríguez-Carvajal, Physica B **192**, 55 (1993).
[14]M. Guc, S. Levcenko, V. Izquierdo-Roca, X. Fontane, E. Arushanov, and A. Pérez-Rodríguez, J. Appl. Phys. **114**, 193514 (2013).
[15]J. G. Albornoz, R. Serna, and M. Leon, J. Appl. Phys. **97**, 103515 (2005).
[16]D. E. Aspnes and A. A. Studna, Appl. Opt. **14**, 1131 (1975).
[17]T. Kawashima, S. Adachi, H. Miyake, and K. Sugiyama, J. Appl. Phys. **84**, 5202 (1998).
[18]A. Corana, M. Marchesi, C. Martini, and S. Ridella, ACM Trans. Math. Software **13**, 262 (1987).
[19]A. B. Djurisic and E. H. Li, Appl. Phys. A **73**, 189 (2001).
[20]S. Levcenko, L. Duran, G. Gurieva, M. I. Alonso, E. Arushanov, C. A. Durante Rincón, and M. León, J. Appl. Phys. **107**, 033502 (2010).
[21]M. León, S. Levcenko, R. Serna, A. Nateprov, G. Gurieva, J. M. Merino, S. Schorr, and E. Arushanov, Mater. Chem. Phys. **141**, 58 (2013).
[22]M. I. Alonso, K. Wakita, J. Pascual, M. Garriga, and N. Yamamoto, Phys. Rev. B **63**, 075203 (2001).
[23]F. Luckert, D. I. Hamilton, M. V. Yakushev, N. S. Beattie, G. Zoppi, M. Moynihan, I. Forbes, A. V. Karotki, A. V. Mudryi, M. Grossberg, J. Krustok, and R. W. Martin, Appl. Phys. Lett. **99**, 062104 (2011).
[24]M. León, S. Levcenko, A. Nateprov, A. Nicorici, M. Merino, R. Serna, and E. Arushanov, J. Phys. D **40**, 740 (2007).